

## Neck Length and Processivity of Myosin V\*

Received for publication, April 8, 2003, and in revised form, May 9, 2003  
Published, JBC Papers in Press, May 11, 2003, DOI 10.1074/jbc.M303662200

Takeshi Sakamoto<sup>‡</sup>, Fei Wang<sup>‡</sup>, Stephan Schmitz<sup>§</sup>, Yuhui Xu<sup>¶</sup>, Qian Xu<sup>‡</sup>, Justin E. Molloy<sup>§</sup>,  
Claudia Veigel<sup>§</sup>, and James R. Sellers<sup>‡||</sup>

From the <sup>‡</sup>Laboratory of Molecular Cardiology and <sup>¶</sup>Electron Microscopy Core, NHLBI, National Institutes of Health, Bethesda, Maryland 20892-1762 and <sup>§</sup>Division of Physical Biochemistry, National Institutes for Medical Research, London NW71AA, United Kingdom

**Myosin V is an unconventional myosin that transports cargo such as vesicles, melanosomes, or mRNA on actin filaments. It is a two-headed myosin with an unusually long neck that has six IQ motifs complexed with calmodulin. *In vitro* studies have shown that myosin V moves processively on actin, taking multiple 36-nm steps that coincide with the helical repeat of actin. This allows the molecule to “walk” across the top of an actin filament, a feature necessary for moving large vesicles along an actin filament bound to the cytoskeleton. The extended neck length of the two heads is thought to be critical for taking 36-nm steps for processive movements. To test this hypothesis we have expressed myosin V heavy meromyosin-like fragments containing 6IQ motifs, as well as ones that shorten (2IQ, 4IQ) or lengthen (8IQ) the neck region or alter the spacing between 3rd and 4th IQ motifs. The step size was proportional to neck length for the 2IQ, 4IQ, 6IQ, and 8IQ molecules, but the molecule with the altered spacing took shorter than expected steps. Total internal reflection fluorescence microscopy was used to determine whether the heavy meromyosin IQ molecules were capable of processive movements on actin. At saturating ATP concentrations, all molecules except for the 2IQ mutant moved processively on actin. When the ATP concentration was lowered to 10  $\mu$ M or less, the 2IQ mutant demonstrated some processive movements but with reduced run lengths compared with the other mutants. Its weak processivity was also confirmed by actin landing assays.**

The myosin superfamily consists of at least 18 classes of actin-dependent molecular motors (1). Class V myosins transport cargos such as endoplasmic reticulum in neurons, melanosomes in melanocytes, and mRNA in yeast (2). Similar to other myosins, they are composed of a head that binds ATP and actin and a neck region consisting of calmodulin (CaM)<sup>1</sup> molecules bound to an  $\alpha$ -helical segment of the myosin heavy chain. The C-terminal tail domain of myosin V has coiled-coil forming motifs that dimerize and create two-headed molecules but do not self-associate into filamentous structures. The IQ motifs of

the heavy chain, implicated in the binding of CaM or light chain subunits, have the consensus sequence, IQXXXRGXXXR, where X is any amino acid (3). The neck of mouse myosin V has six IQ motifs, each of which binds CaM, making its neck longer than that of most myosins (4). The six IQ motifs of all myosin V superfamily members are separated by 25–23–25–23–25 amino acids.

The well studied myosin II class molecules that power muscle contraction and participate in cytokinesis in nonmuscle cells polymerize into filaments that are interdigitated with actin filaments. Kinetic and mechanical studies have demonstrated that these myosins interact only transiently with actin and typically spend greater than 95% of their kinetic cycle detached from actin. The term “low duty cycle” motor has been used to describe this behavior adopted to allow the sliding of actin filaments past myosin filaments to be unimpeded by nonproductive strongly bound myosin heads that have completed their powerstroke.

If a vesicle translocating myosin had similar kinetics, a patch of 20 or more myosins would have to be positioned to possibly interact with actin to keep the vesicle attached to the actin filament so that it could move processively. Alternatively, if the myosin ATPase kinetics were altered such that the myosin spent most of its kinetic cycle strongly bound to actin, then a small number or possibly even a single myosin could efficiently translocate its vesicle processively along an actin filament. Another consideration for vesicle movement is that the actin filament is a helical polymer composed of 5 nm monomers with a 36-nm half-repeat that is usually bound to the cytoskeleton. If the moving myosin stepped from one actin monomer to the next, the motor and vesicle would rotate around the actin filament and crash its cargo into the cytoskeleton before any appreciable distance could be covered. Alternatively, if the motor could take large steps that matched the actin pseudo-repeat, it could effectively walk across the “top” of the cytoskeletal-bound actin filament while holding its cargo above.

Experiments using optical trapping nanometry, electron microscopy, and single molecule motility studies demonstrated that myosin V moves processively along actin filaments, taking many 36-nm steps before dissociating (5–8). Kinetic analyses demonstrated that it is a high duty cycle motor that associates strongly with actin in the presence of physiological concentrations of ATP (9). The processive nature and long step size reflect the intracellular function of the molecule as a cargo motor. The processivity is necessary to keep the cargo tethered to the actin filament, whereas the long step size matches the pseudo-repeat of the actin filament, allowing myosin V to “walk” across the top of, rather than rotate around, the actin filament, which would occur if the molecule took steps either longer or shorter than 36 nm. This behavior is in marked contrast to the myosin II molecules that power muscle contrac-

\* The costs of publication of this article were defrayed in part by the payment of page charges. This article must therefore be hereby marked “advertisement” in accordance with 18 U.S.C. Section 1734 solely to indicate this fact.

|| To whom correspondence should be addressed: Bldg. 10, Rm. 8N202, NHLBI, National Institutes of Health, Bethesda, MD 20892-1762. Tel.: 301-496-6887; Fax: 301-402-1542; E-mail: sellersj@nhlbi.nih.gov.

<sup>1</sup> The abbreviations used are: CaM, calmodulin; HMM, heavy meromyosin; WT, wild type; TIRF, total internal reflection fluorescence; MOPS, 4-morpholinepropanesulfonic acid; TEMED, *N,N,N',N'*-tetramethylethylenediamine; TES, 2-[[2-hydroxy-1,1-bis(hydroxymethyl)ethyl]amino]ethanesulfonic acid.

tion. These low duty ratio myosins are designed to make single transient interactions with actin and spend most of their kinetic cycle dissociated from actin (10, 11).

To test whether the long neck is essential for processive movement and how neck length affects the working stroke, we engineered recombinant heavy meromyosin (HMM)-like myosin V molecules with shorter or longer necks than that of wild type (WT) myosin V HMM by altering the number of IQ motifs. The effect of neck length on step size was measured in an optical trap, and the processivity was measured by directly observing the movements of single, fluorescently labeled molecules on actin using total internal reflection fluorescence (TIRF) microscopy. The results strongly suggest that a neck containing more than two CaM subunits is necessary for efficient processive movement, and the step size is roughly proportional to the length of the neck.

#### EXPERIMENTAL PROCEDURES

**Construction of Myosin V HMM-IQ Mutant**—Mouse myosin V HMM-like and S1-like WT fragments were as described previously (12). The HMM-6IQ cDNA in baculovirus transfer vector pVL1392 was used to subclone the IQ mutants using a PCR-based strategy. The arrangements of the IQ motifs in the final products are as depicted in Fig. 1. Recombinant baculoviruses were produced as described previously (12).

**Preparations of Proteins**—HMM-IQ molecules were co-expressed with CaM in baculovirus/Sf9 cells and purified using FLAG-affinity chromatography (12). The concentration of purified WT and IQ mutants were measured using the following extinction coefficients ( $A_{280}-A_{320}$ ) calculated from their cDNA sequences: S1-6IQ, 0.644; HMM-2IQ, 0.683; HMM-4IQ, 0.631; HMM-6IQ, 0.607; HMM-8IQ, 0.591; HMM-2Ala-6IQ, 0.607. All values are for  $e^{1 \text{ mg/ml}}$ . Biotin labeling of actin, Alexa 488 labeling of CaM, and exchange of Alexa 488-CaM into the HMM-IQ constructs were performed as described previously (6). Actin was purified from skeletal muscle (13). Rhodamine-phalloidin-labeled rabbit F-actin and *N*-ethylmaleimide-modified rabbit myosin were prepared by standard methods (14). Rabbit skeletal muscle HMM was prepared according to Homsher *et al.* (15).

**MgATPase Assay**—The MgATPase activity was measured using an NADH-coupled assay at 25 °C in 10 mM MOPS, pH 7.0, 2 mM MgCl<sub>2</sub>, 1 mM ATP, 50 mM KCl, 0.15 mM EGTA, 40 units/ml *l*-lactic dehydrogenase, 200 units/ml pyruvate kinase, 200 μM NADH, and 1 mM phospho(enol)pyruvate.  $V_{\text{max}}$  and  $K_{\text{ATPase}}$  were obtained by fitting the data to the Michaelis-Menten equation.

**In Vitro Motility Assays**—The motility assay was performed and quantified as described previously in a motility buffer containing 20 mM MOPS, pH 7.4, 2 mM MgCl<sub>2</sub>, 0.1 mM EGTA, 50 mM KCl, 1 mM ATP, 1 μM CaM, 25 μg/ml glucose oxidase, 45 μg/ml catalase, 2.5 mg/ml glucose, and 50 mM dithiothreitol at 30 °C (12, 15).

The TIRF assay was performed on an Olympus IX70 microscope equipped for objective type TIRF using a PlanApo (×60, numerical aperture 1.45) objective lens and a relay lens (PE5, ×5 or PE2.5, ×2.5; Olympus) connected to an image-intensified (KS1380; Videoscope) neuveon camera (model C2400; Hamamatsu Photonics). Excitation light sources were an argon laser (488 nm, model 163-C0201; Spectra Physics) and a diode green laser (532 nm, model GCC-025-C; Crystal Laser). To prevent nonspecific binding of fluorescently labeled-protein, the coverslips (top, 18 × 18 mm and bottom, 24 × 50 mm) comprising the flow cell were prepared as follows. Coverslips were soaked in 5 N NaOH for 2 days, washed extensively with warm water, and placed into a sealed plastic box containing an open Eppendorf tube of acryloyl silanes (prepared by mixing 3-methacryloxypropyltrimethoxy-silane (Sigma) and 3-aminopropyltriethoxysilane (Pierce) in a 10:1 ratio) for 1 h at 50 °C. Unbound silane was removed by a brief rinse in 100% methanol. A solution of 2% acrylamide, 0.5% bisacrylamide, 0.1% cystamine, 0.1% ammonium persulfate, and 1% TEMED, was dropped onto the silane-coated coverslips, which were then inverted and placed on top of a 25 × 100-mm microscope slide with the wet surface adhering to the slide. After 45 min at 37 °C the coverslip and slide were separated with a razor, and unbound acrylamide and cystamine were washed away by filtered (0.45-μm pore diameter) deionized water (dH<sub>2</sub>O). Coverslips were then immersed in 1% 2-mercaptoethanol for 15 min to reduce disulfide bonds in the cystamine and then washed with a gentle flow of filtered dH<sub>2</sub>O. Biotin-maleimide (2 mM) in 20 mM TES, pH 7.0, was dropped onto the acrylamide-coated coverslip and incubated for 4 h at 37 °C. Upper coverslips (18 × 18 mm) were treated the same as the

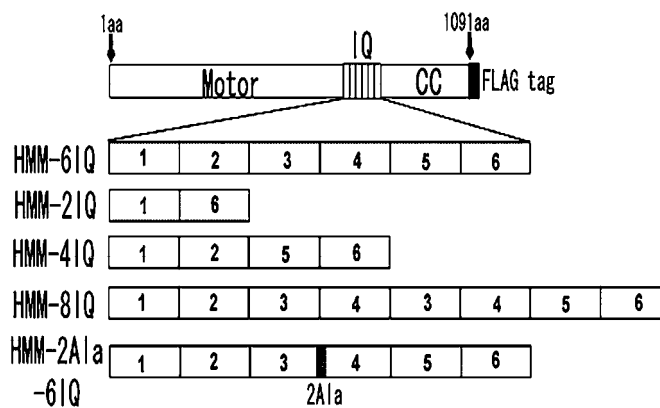


FIG. 1. Schematic diagrams of HMM-IQ molecules. Myosin V HMM heavy chain consists of a motor domain, a neck domain containing six IQ motifs, and a coiled-coil tail (CC). To facilitate purification, a FLAG tag (black box) was attached to the C terminus. HMM-2Ala-6IQ has two additional Ala residues between the 3rd and 4th IQ motifs.

bottom one except that no cystamine was used. The flow cell, 15 μl in volume, was prepared using double-sticky cellophane tape. For TIRF assays, 30 μl streptavidin (47 μg/ml) solution was applied to the flow cell, incubated for 4 min, and washed with motility assay buffer (1 ml). Biotin-labeled, rhodamine-phalloidin-labeled rabbit F-actin filaments (1 μM) were applied to the flow cell and incubated for 2 min. Unbound actin was washed off with 1 ml of motility assay buffer. Fluorescently labeled HMM in 100 μl of motility assay buffer containing 1 μM CaM was introduced into the flow cell, which was then mounted onto the microscope for imaging. Data were captured on a sVHS videotape, and the run length and the velocity of single fluorescently labeled myosin V HMM molecules were measured using MetaMorph (Universal Imaging).

Landing assays were performed in the motility assay buffer described above, except containing 2 mM ATP (5). The sample was illuminated by laser at an angle less than the critical angle for TIRF to produce conditions in which higher concentrations of rhodamine-phalloidin-labeled rabbit F-actin (21 μg/ml) could be used than with conventional epifluorescence illumination, yet actin filaments could be imaged farther away from the surface than when using conventional TIRF.

**Optical Trapping Conditions**—The optical trapping apparatus, detection, and quantification of events and solution conditions were as described previously (8, 14, 16). In brief, a single actin filament was captured between two *N*-ethylmaleimide-myosin coated latex beads (1 μm diameter) held in two independent optical traps. The actin was positioned over a third surface-bound bead that was sparsely coated with HMM-IQ molecules. The surface density was adjusted by serial dilution of the HMM-IQ solutions such that only one in three beads gave binding events. Mechanical interactions were measured by monitoring the positions of the beads holding the actin filament using two photodetectors (14).

**Electron Microscopy**—Rotary shadowed images of HMM-IQ mutants were obtained as described previously (12, 17).

#### RESULTS

**Characterization of Expressed Myosin IQ Mutant**—To examine the role of the myosin V neck in its ability to take long steps and move processively on actin, recombinant HMM-like fragments were engineered in which IQ motifs in the neck region of myosin V were deleted, added, or modified. The common structural elements of the myosin V IQ mutants are an N-terminal motor domain and a C-terminal coiled-coil region. The number of IQ motifs for each mutant varied according to Fig. 1. One mutant retained all IQ motifs but had two alanine residues inserted between the 3rd and 4th motifs (HMM-2Ala-6IQ). This mutation alters the regular 25/23 amino acid repeating pattern between adjacent IQ motifs common to all myosin V members and thus may alter the flexibility or orientation of the neck (Fig. 2a).

The electrophoretic mobility of the HMM-IQ mutants varied in proportion to the number of IQ motifs (Fig. 2b). Rotary

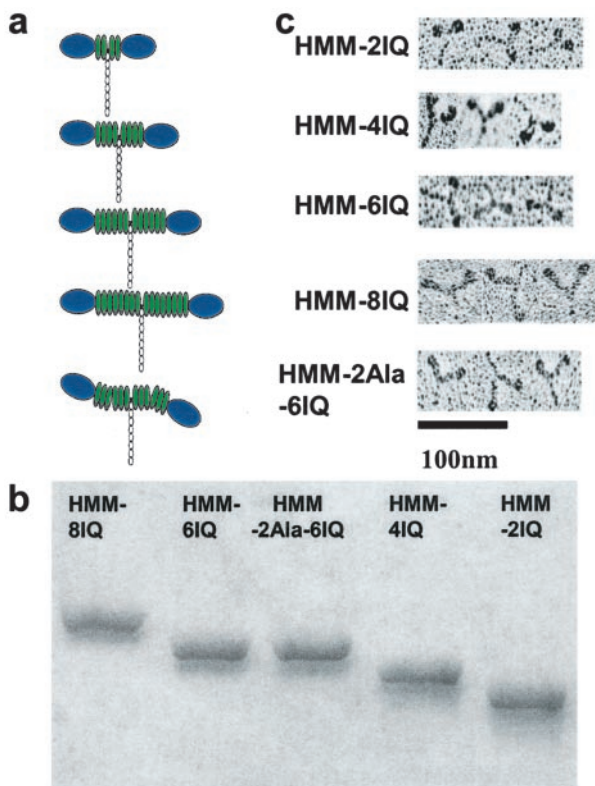


FIG. 2. Characterization of expressed HMM-IQ molecules. *a*, schematics of HMM-IQ molecules. The neck of HMM-2Ala-6IQ is depicted as bent between the 3rd and 4th IQ motifs although this is not routinely observed in the rotary shadowed images. *b*, 6% SDS-PAGE gel of HMM-IQ molecules showing their heavy chains. *c*, rotary shadowed electron microscopic images of HMM-IQ molecules. Scale bar, 100 nm.

shadowed electron microscopic images of the molecules were consistent with the neck lengths, but no obvious differences were observed between the images of HMM-2Ala-6IQ and HMM-6IQ in terms of neck flexibility (Fig. 2*c*).

**ATPase Activity**—The steady-state MgATPase at various actin concentrations was measured using an NADH-coupled assay to prevent ADP build up. The MgATPase activities of all HMM-IQ constructs were  $<0.02 \text{ s}^{-1}$  in the absence of actin and were activated  $\sim 750$ -fold by actin (Table I). The  $V_{\text{max}}$  of myosin V S1-6IQ ( $15.3 \text{ s}^{-1}$ ) was consistently higher than that of all HMM-IQ molecules (between 10 and  $12 \text{ s}^{-1} \text{ head}^{-1}$ ). The  $K_{\text{ATPase}}$  of HMM-6IQ (WT), HMM-8IQ, and HMM-2Ala-6IQ were slightly lower than that of HMM-2IQ and HMM-4IQ, whereas that of myosin V S1-6IQ was much higher than those of the HMM constructs.

**Sliding Actin In Vitro Motility Assay**—*In vitro* actin sliding assays under conditions where multiple HMM molecules can interact with actin showed that the velocity increased with increasing neck length for the HMM-2IQ, HMM-4IQ, HMM-6IQ, and HMM-8IQ (Table I). The velocity of HMM-2Ala-6IQ was intermediate between that of HMM-2IQ and HMM-4IQ. The velocity of S1 was slower than that of HMM-6IQ (Table I) (12).

**Optical Trapping**—The mechanical properties of the HMM-IQ constructs undergoing single step interactions with actin were observed using a dual optical trapping apparatus (8) (Fig. 3). The amplitudes of single displacement events of HMM-2IQ, HMM-4IQ, HMM-6IQ, and HMM-8IQ were proportional to neck length. The displacements for HMM-4IQ and HMM-6IQ were similar to those observed for S1-4IQ and S1-6IQ constructs (18), suggesting that they represent the working stroke produced by a single head. HMM-2Ala-6IQ gave a sig-

nificantly shorter step size than expected from its neck length, which may be because of extra flexibility in the lever arm caused by the insertion of the two alanines (Fig. 3). The lifetimes of attachment ( $t_{50}$ ) for all constructs were about 0.22 s at  $5 \mu\text{M}$  ATP.

**Landing Assay**—The actin landing rate, a measure of how many actin filaments land on the surface in a given period of time and move longer than  $0.2 \mu\text{m}$  as the myosin surface density is decreased, distinguishes between processive motors requiring only a single myosin molecule to move actin filaments and nonprocessive ones requiring multiple myosins to translocate actin filaments (5). The data of HMM-6IQ, HMM-4IQ, HMM-8IQ, and HMM-2Ala-6IQ were well fitted with  $n = 1$  for the landing equation, consistent with these molecules being processive motors (Fig. 4). In contrast, the data for HMM-2IQ was fitted with an  $n = 2$  suggesting that this molecule is not processive. Myosin V S1-6IQ and skeletal muscle HMM did not support movement at surface densities less than 3000 and 9000 molecules/ $\mu\text{m}^2$  and were fitted by  $n = 3$  and  $n = 6$ , respectively (Fig. 4). At very low surface density (less than 20 molecules per  $\mu\text{m}^2$ ), HMM-4IQ, HMM-6IQ, HMM-8IQ, and HMM-2Ala-6IQ supported movement of landed actin filaments, but the moving filaments often pivoted about a single attachment point as described for intact myosin V and kinesin at low surfaces densities (5, 12, 19). This behavior was not seen for HMM-2IQ and S1-6IQ.

**Single Molecule Motility Assay (TIRF Assay)**—The endogenous CaMs of HMM-IQ mutants were partially exchanged for Alexa-488-labeled CaM, and single-fluorescently labeled HMM-IQ molecules were visualized using TIRF microscopy (6). The ratio between the fluorescence intensity and the HMM concentration in solution was used to determine the average number of fluorophores per HMM molecule, and the quantal photobleaching characteristics of the individual fluorescent molecules bound to the surface were then measured as a function of time (data not shown). The labeling ratio of all HMM-IQ constructs corresponded to the average number of photobleaching events observed in single spots in TIRF microscopy, suggesting that each fluorescent spot is a single HMM molecule. The average number of photobleaching events did not increase linearly with the number of IQ motifs of the HMM-IQ constructs (HMM-2IQ, 3.1 events; HMM-4IQ, 3.1; HMM-6IQ, 4.5; HMM-8IQ, 6.0; S1, 2), suggesting that not all CaMs exchange uniformly.

Single HMM-6IQ molecules bound to and moved in a highly processive manner along actin filaments bound to the surface, often moving all the way to the end of the actin filament before detaching (Fig. 5*a*). Fig. 5*b* plots the “full run frequency” defined as the probability that, upon attachment, an HMM molecule moves all the way to the end of the actin filament without detachment. The mean length of the actin filaments bound to the surface is  $4.3 \pm 2.5 \mu\text{m}$ . At 25 mM KCl and 2 mM ATP, the full run frequency for HMM-6IQ was about 80% (Fig. 5*b*). Under the same conditions, HMM-4IQ, HMM-8IQ, and HMM-2Ala-6IQ also moved highly processively with full run frequencies of more than 50%. In marked contrast, almost no HMM-2IQ molecules were able to move the entire remaining length of the actin filament under these conditions. When the ATP concentration in the assay was lowered, the full run frequency increased for all of the HMM-IQ molecules. At low ATP concentrations ( $1 \mu\text{M}$  and  $10 \mu\text{M}$ ) even HMM-2IQ exhibited a significant full run frequency.

Another way to demonstrate the difference between the behaviors of HMM-2IQ and HMM-6IQ is to examine movement frequency, the number of molecules that attach and have detectable movement as opposed to merely attaching and detach-

TABLE I  
Properties of the expressed myosin V HMM-IQ molecules

Myosin V Mutants	S1-6IQ	HMM-2IQ	HMM-4IQ	HMM-6IQ	HMM-8IQ	HMM-2Ala-6IQ
$V_{\max}$ ( $s^{-1}$ per head)	$15.3 \pm 4.3$	$10.8 \pm 2.6$	$12.4 \pm 1.9$	$9.7 \pm 1.0$	$10.5 \pm 1.6$	$10.2 \pm 1.4$
$K_{ATPase}$ ( $\mu M$ )	$3.6 \pm 1.0$	$0.64 \pm 0.17$	$0.88 \pm 0.12$	$0.32 \pm 0.09$	$0.37 \pm 0.12$	$0.26 \pm 0.10$
Actin sliding velocity ( $\mu m/s$ )	$0.20 \pm 0.03^a$	$0.29 \pm 0.07$	$0.36 \pm 0.08$	$0.38 \pm 0.09$	$0.43 \pm 0.12$	$0.31 \pm 0.13$

<sup>a</sup> Experiments carried out at 40 mM KCl.

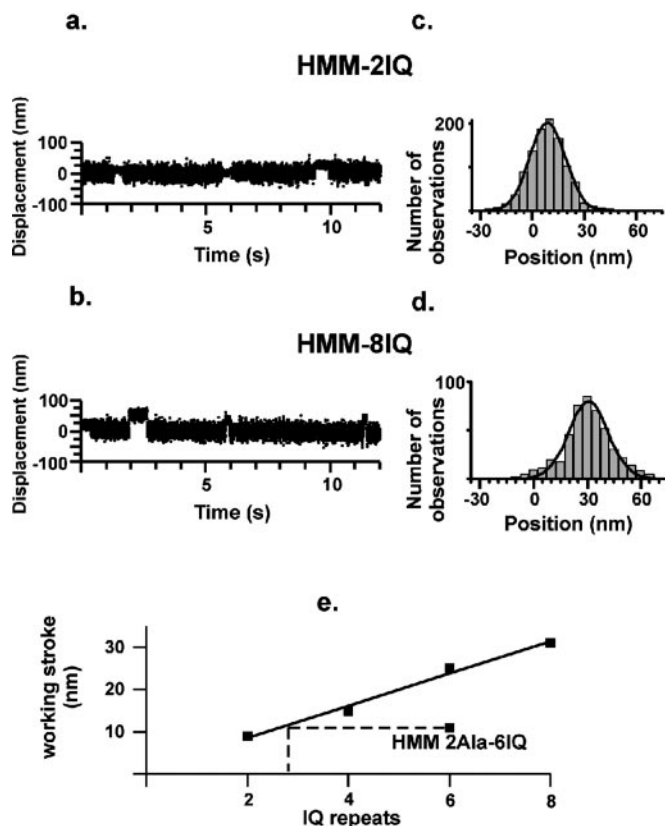


FIG. 3. Single-molecule mechanical interactions measured for the HMM-IQ mutants using optical tweezers. *a* and *b*, records showing bead movement in parallel with the actin filament axis. Intervals of reduced Brownian noise indicate attachment events of HMM-2IQ (*a*) and HMM-8IQ (*b*). *c* and *d*, amplitude of single step displacements; HMM-2IQ mean  $\pm$  S.E.,  $8.9 \pm 0.3$  nm,  $n = 1058$ ,  $t_{50}$  ( $5 \mu M$  ATP) =  $0.228$  s (*c*); HMM-8IQ  $30.7 \pm 0.5$  nm,  $n = 473$ ,  $t_{50}$  ( $5 \mu M$  ATP) =  $0.206$  s (*d*). *e*, effect of lever arm length on working stroke size; HMM-2IQ mean  $\pm$  S.E.,  $6.2 \pm 0.6$  nm,  $n = 232$ ,  $t_{50}$  ( $5 \mu M$  ATP) =  $0.225$  s; HMM-2Ala-6IQ  $10.9 \pm 0.6$  nm,  $n = 213$ ,  $t_{50}$  ( $5 \mu M$  ATP) =  $0.24$  s; HMM-4IQ  $15.4 \pm 0.5$  nm,  $n = 1003$ ,  $t_{50}$  ( $5 \mu M$  ATP) =  $0.228$  s; HMM-6IQ  $25.2 \pm 0.6$  nm,  $n = 1967$ ,  $t_{50}$  ( $5 \mu M$  ATP) =  $0.243$  s. For conditions see “Experimental Procedures.”

ing. At 25 mM KCl and  $10 \mu M$  ATP, only 7% of the HMM-2IQ molecules that attached to actin moved, whereas 98% of the HMM-6IQ molecules that bound to actin moved (Table II). At the same KCl concentration and 2 mM ATP, greater than 99% of the HMM-6IQ molecules that attached to actin moved, whereas in the same observation period no movement events were observed for HMM-2IQ. Fig. 5, *c-h* shows a distribution of the actual measured run lengths. This distribution will be blunted for a highly processive motor as its run length will be limited by the available length of the actin filament. The bar on the far left represents HMM molecules that attached but moved less than 200 nm. At 25 mM KCl, all of the HMM-IQ molecules except the HMM-2IQ exhibited long processive runs ( $>0.5 \mu m$ ). The mean run length of HMM-6IQ ( $1.81 \mu m$ ) was longer than that of HMM-4IQ ( $0.74 \mu m$ ), HMM-8IQ ( $1.38 \mu m$ ), and HMM-2Ala-6IQ ( $0.76 \mu m$ ). HMM-2IQ exhibited some movements longer than 200 nm, but the frequency was low, and the length of the

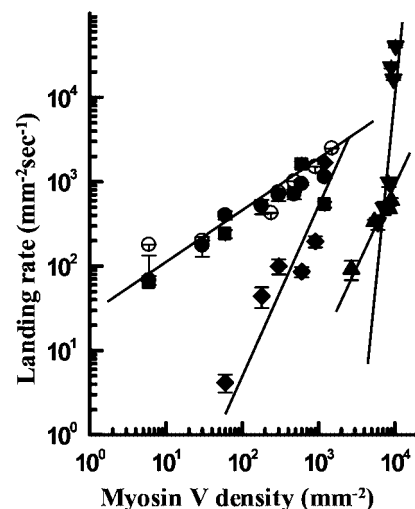


FIG. 4. Actin filament landing assay. The numbers of actin filaments that bound to the surface and moved for at least  $0.2 \mu m$  were scored. The symbols are as follows: HMM-2IQ, diamond; HMM-4IQ, square; HMM-6IQ, open circle; HMM-8IQ, closed circle; myosin V S1-6IQ, triangle; and skeletal muscle HMM, inverted triangle. The landing rate data of HMM-6IQ, HMM-4IQ, and HMM-8IQ were fitted by the theoretical curve where  $n = 1$  as described in Mehta *et al.* (5). The landing rate data of HMM-2Ala-6IQ were also fitted by  $n = 1$  (data not shown). The data for HMM-2IQ, myosin V S1-6IQ, and skeletal muscle HMM were fitted by  $n = 2, 3$ , and 6, respectively. The assay contained 25 mM KCl and 2 mM ATP.

run was typically shorter (Fig. 5, *a* and *c*). At 100 mM KCl concentration very few processive movements were seen for HMM-4IQ (Fig. 5*e*), but HMM-6IQ and HMM-8IQ molecules still showed long processive run lengths (data not shown).

The velocity of single HMM-IQ mutants on actin filaments in the TIRF assay was roughly proportional to neck length at  $10 \mu M$  ATP (Fig. 6). However at 2 mM ATP, single molecules of HMM-6IQ moved faster than any other mutant, including the HMM-8IQ. No movements of HMM-2IQ were observed under these conditions, and HMM-2Ala-6IQ moved slower than HMM-6IQ.

Single myosin V S1-6IQ molecules could bind to actin filaments, but no movements were observed (Fig. 7). The attachment lifetime at 2 mM ATP (0.12 s) is shorter than that at  $1 \mu M$  ATP concentration (0.52 s). The value at 2 mM ATP is consistent with the  $V_{\max}$  of the actin-activated Mg-ATPase and the expected dwell time (0.11 s) from Tanaka *et al.* (20) if S1 is not a processive molecule. At  $1 \mu M$  ATP the lifetime is longer as expected for a second order reaction at low substrate concentration.

## DISCUSSION

Myosin V molecules have six IQ motifs that are always separated by 25-23-25-23-25-23 amino acids, respectively. The extended neck allows the myosin V to take long steps that match the pseudo-repeat of the actin filament (5, 7, 8). In doing so, myosin V should keep its cargo positioned above the cytoskeleton while stepping from one actin filament crossover point to the next. To determine how the length of the neck affected the mechanical properties of the myosin and whether

**FIG. 5. Run lengths of HMM-IQ molecules.** *a*, time series showing processive movements of individual fluorescently labeled myosin V HMM-6IQ (*right panel*) and HMM-2IQ (*left panel*) on actin filaments. Note the difference in time scales. The *arrow* and *arrowhead* indicate the positions of individual myosin molecules that are moving on actin. *Scale bar*, 2  $\mu\text{m}$ . The assay buffers contained 25 mM KCl for both samples whereas the HMM-6IQ sample contained 2 mM ATP, and the HMM-2IQ contained 10  $\mu\text{M}$  ATP. *b*, full run length percentage plot at various ATP concentrations. *Bars* show the percentage of HMM molecules that bind to an actin filament and then move to the very end without detaching. HMM-2IQ, *filled bars*; HMM-4IQ, *open bars*; HMM-6IQ, *diagonally down shading*; HMM-8IQ, *horizontal shading*; and HMM-2Ala-6IQ molecules, *diagonally up shading*. *c-h*, distribution of run lengths on actin tracks by individual HMM-IQ molecules. *Solid curves*, exponential fit with run length constants as follows: *c*, 229 nm; *d*, 1380 nm; *e*, 58 nm; *f*, 738 nm; *g*, 763 nm; *h*, 1810 nm.

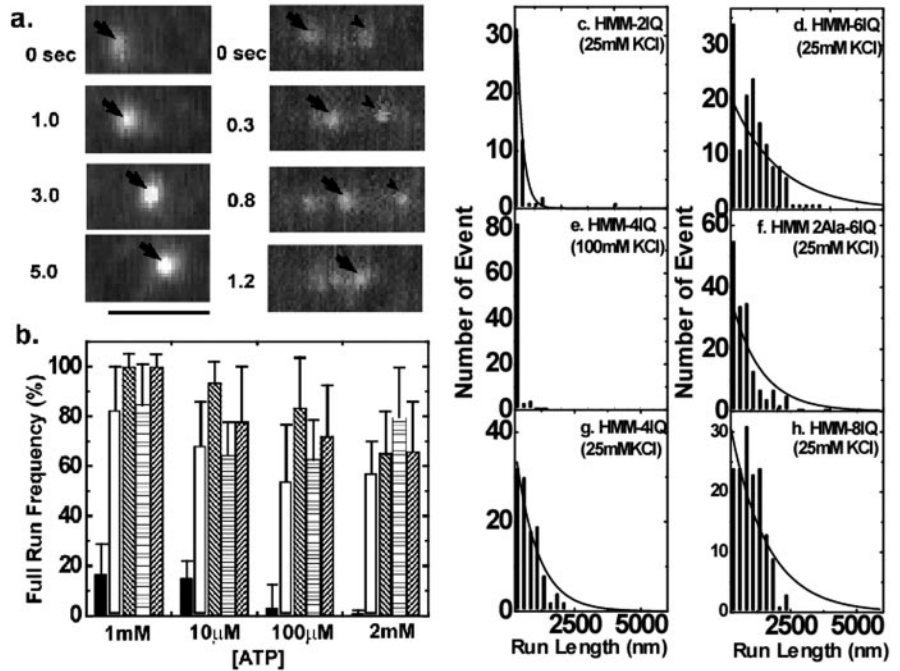


**TABLE II**  
Percentage of attached HMM-IQ molecules that moved

Myosin V mutant	10 $\mu\text{M}$ ATP	2 mM ATP
HMM-2IQ	7	0
HMM-6IQ	98	99

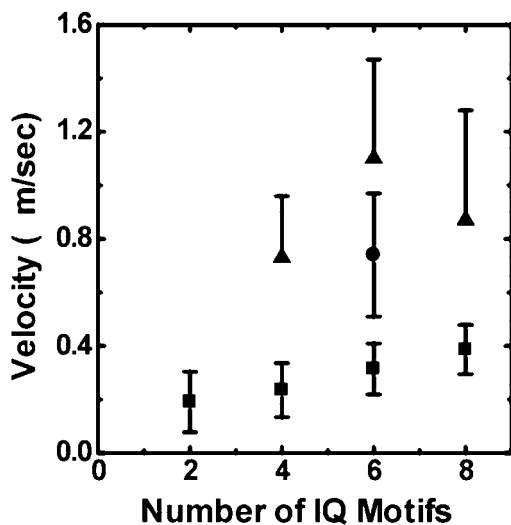


**FIG. 6. The rate of single molecules of HMM-IQ molecules moving processively on actin filaments.** *Square*, 25 mM KCl, 10  $\mu\text{M}$  ATP; *triangle*, 100 mM KCl, 2 mM ATP; *circle*, HMM-2Ala-6IQ at 100 mM KCl and 2 mM ATP. *Data points* are the average of 65 to 140 different movement events.

a long neck was a requirement for processive movement on actin filaments, we expressed myosin V HMM molecules that had two, four, six, or eight IQ motifs in the neck. Another contained all six IQ motifs, but altered the spacing between the 3rd and 4th IQ motifs by the insertion of two alanine residues. Mouse myosin V that has only CaM as light chains has advantages over similar experiments performed earlier with either myosin II molecules or chicken myosin V that have two types of lights chains bound to the IQ motifs (12, 18, 21, 22).

Two different assays were used to probe whether the neck

length affected processivity. One involved watching single fluorescently labeled HMM-IQ molecules interact with actin using TIRF microscopy. At 100 mM KCl and 2 mM ATP only the WT HMM-6IQ and the HMM-8IQ showed long processive movements. When the KCl concentration was lowered to 25 mM, the HMM-4IQ also moved processively for significant distances. The only conditions in which HMM-2IQ showed significant processive movements in the TIRF assay were at very low ATP concentrations (1 and 10  $\mu\text{M}$  ATP) and at low ionic strength. Even here, the frequency with which HMM-2IQ moved on actin filaments was markedly lower than with the other mutants. The lack of robust processivity of HMM-2IQ cannot be attributed to the geometry of the assay. Purcell *et al.* (18) used optical tweezers to measure the step size of a myosin V HMM-4IQ construct undergoing processive movements and found a value of 25 nm compared with 36 nm obtained from the WT HMM-6IQ. They proposed that the two heads of HMM-4IQ must bind to actin monomers 25 nm apart and be rotated about 90° around the actin filament. For this molecule to move processively, it would have to rotate around the actin filament in a right-handed direction or meander between the two strands as it advanced. In our experiments, actin filaments are bound to a streptavidin-coated surface via biotin-groups coupled to actin. By varying the ratio of unlabeled to biotin-labeled actin in a filament, we vary the tightness with which the filament is tacked down to the surface. The processivity of HMM-4IQ and HMM-8IQ dramatically decreases when the ratio of unlabeled actin to biotinylated actin decreases from 100:1 to 10:1, whereas the processivity of HMM-6IQ is not affected (data not shown). This suggests that the former group of molecules must rotate around the actin filament to some extent to move processively and that this rotation is inhibited if the actin filaments are tightly tacked down. The low frequency of processive movements observed with the HMM-2IQ, however, is probably not due to steric hindrance of the expected rotation because of the actin filament being tightly tacked down to the surface, since HMM-4IQ molecules move processively under these conditions.

Another way of addressing processivity is to measure the landing rate of actin filaments as a function of myosin surface density. When the experimental data were fitted to an equation

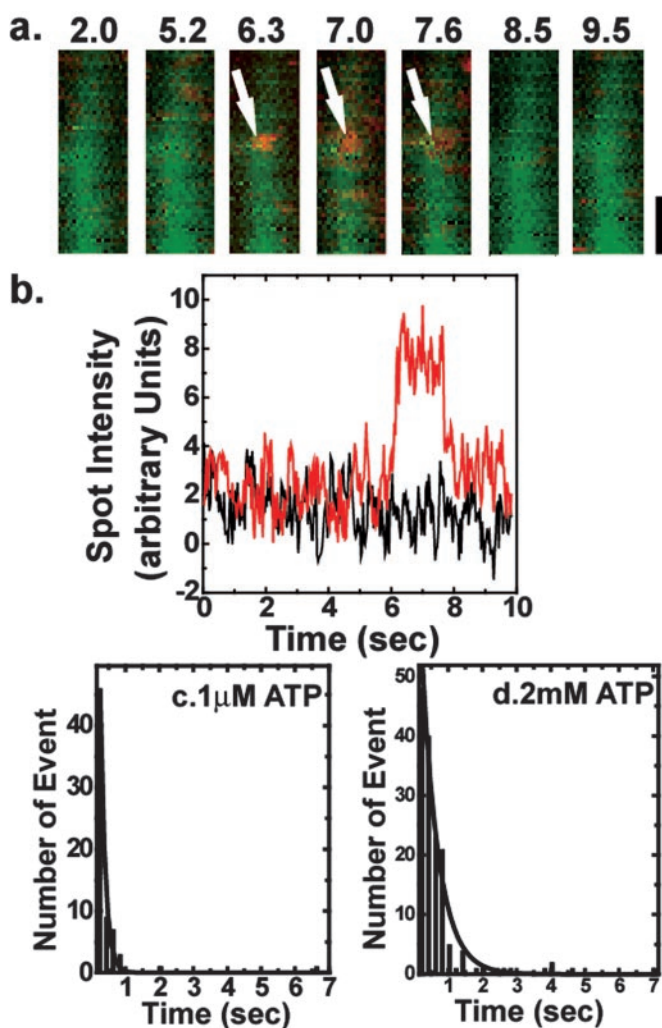


FIG. 7. **Myosin V S1-6IQ does not move processively.** *a*, time series showing attachment and detachment of a myosin V S1-6Q molecule (red spot) to an actin filament (green) using TIRF microscopy. The numbers at the top of the image panels correspond to the *x*-axis in *b*. Scale bar, 1  $\mu\text{m}$ . *b*, fluorescence intensity (solid red line) of fluorescently labeled myosin V S1-6IQ on the actin track at 1  $\mu\text{M}$  ATP. The intensity of an individual fluorescent spot is plotted against time. The solid black line is background fluorescence from a similar area. *c* and *d*, attachment life times of myosin V S1-6IQ molecules at 1  $\mu\text{M}$  (*c*) and 2 mM ATP (*d*). Solid curves, exponential fits with lifetimes as follows: *c*, 0.52 s; *d*, 0.12 s.

derived to determine the minimal number of molecules,  $n$ , required to translocate an actin filament, the HMM-2IQ data were best fit to an  $n$  of 2, whereas the other HMM-IQ molecules showed an  $n$  of 1. Thus a neck length of greater than 2IQ motifs is required for efficient processive movements.

The size of single displacements measured using optical tweezers and the rate of actin filament sliding at moderate myosin V surface densities were roughly proportional to the number of IQ motifs with the exception of HMM-2Ala-6IQ, which moved more slowly and showed smaller single displacements than did the HMM-6IQ. The insertion of two amino acids into a helical segment should result in a 200° rotation of the next IQ motif, which would likely change the normal CaM-CaM interactions and possibly create a less rigid neck.

The rate of movement of single molecules of each mutant was measured at both low (10  $\mu\text{M}$ ) and high ATP (2 mM) concentrations using TIRF microscopy. At 2 mM ATP and 100 mM KCl, HMM-6IQ moves faster than HMM-8IQ suggesting that, under unloaded conditions, the rate-limiting process for HMM-8IQ

may be the time to search for a suitable actin binding site. No movements were observed with HMM-2IQ under these conditions. At 10  $\mu\text{M}$  ATP the movement of single molecules of HMM-2IQ, HMM-4IQ, HMM-6IQ, and HMM-8IQ are all roughly proportional to neck length. At this ATP concentration, the ATP binding rate (23) would limit the rate of stepping, and hence velocity would be proportional to neck length (8).

The data above and published experiments (18, 22, 24) have shown that both the working stroke measured from single interactions and the step size obtained when myosin V is moving processively along actin is proportional to the length of the neck region. Interestingly, the rates of movement of vesicles *in vivo* in yeast expressing mutant myosin V molecules were also found to be proportional to neck length (25). Together these studies provide strong support for the lever arm model of myosin motility where the neck region is thought to act as a rigid lever arm in undergoing large scale movements in response to more subtle changes in the motor domain. However, one study with myosin V neck mutants reached a different conclusion. Tanaka *et al.* (20) engineered a chimeric clone with the motor domain and first IQ motif of myosin V fused to the rod of smooth muscle myosin. Trace amounts of this chimera were co-polymerized with skeletal muscle myosin rod fragments. The chimeric myosin V construct showed multiple 36-nm steps per encounter with actin, which the authors interpreted in terms of a model where the neck region does not act as a lever arm. The choice of smooth muscle myosin rod for the chimera may introduce several complexities. First, the N-terminal portion of smooth muscle myosin rod forms a weakly dimerizing coiled-coil (26–28), thus it is possible that even though the chimeric myosin V has a short neck, the coiled-coil smooth muscle S2 segment may be flexible or able to unwind to allow the second head to search for a favorably positioned actin monomer 36 nm away. Second, smooth muscle myosin is thought to assemble via addition of myosin dimers to growing filaments (29, 30). Thus, it is possible that the chimeric myosin was forming dimers consisting of four closely spaced myosin heads when co-polymerizing with skeletal muscle rod fragments, which would increase the likelihood that an actin filament would be moved processively. No other assays for processivity were used in their study. In contrast, we examined processivity using both single molecule motility studies and landing assays. HMM-2IQ was not very processive at high ATP concentrations in either of these assays. A similar conclusion was reached by Purcell *et al.* (18) using HMM-1IQ in their optical trap assays.

Processivity can be viewed as a race between the time needed for the unattached head to find a suitable actin binding site and the ATP cycle time for the attached head. If the bound head dissociates before the unbound head finds a target the myosin dissociates, and the processive run terminates. Veigel *et al.* (8) proposed a model wherein the wild type myosin V spends most of its kinetic cycle attached to actin with a brief stepping time in between periods of two-headed attachment. They further proposed that the kinetic cycles of the two heads are gaited in favor of keeping at least one head attached. Electron microscopic studies show that most of the time the two heads of HMM-6IQ are 13 actin monomers apart (a 36-nm spacing), but some molecules attach with an 11- or 15-actin monomer separation (7) indicating that the leading head has some flexibility in its binding. The virtual lack of processivity of HMM-2IQ at saturating ATP concentrations may be because of a prolonged search time of the unattached head for actin, because we show that its ATP cycling time is not greatly different from that of wild type HMM-6IQ. Because this short neck cannot sample a large landscape, the average time to finding a binding site may

be longer than the cycle time of the bound head at saturating ATP. As the ATP concentration is lowered, the time for binding of ATP to the attached apo head would increase, which might then allow the free head more time to search for a binding site. Thus, the long neck of myosin V may not only have evolved to allow for a powerstroke size coincident with the pseudo-repeat of actin but also to have a high probability of finding a suitable target site.

In summary, our data provide strong support for the lever arm model for myosin movement and demonstrate that the neck length of myosin V has evolved to take advantage of the spacing between actin monomer within the filament. A neck containing six CaM molecules is not absolutely required for processivity, but it is necessary to have a neck with more than two CaMs bound to be able to ensure that at least one head is bound at any given instance under physiological ionic conditions.

*Acknowledgments*—We thank Robert Adelstein for comments on the text and Estelle Harvey and Yue Zhang for excellent technical support. We are especially grateful to Toshio Ando (Kanazawa University, Japan) for advice in preparing the surface for TIRF microscopy.

## REFERENCES

- Sellers, J. R. (1999) *Myosins*, 2nd Ed., Oxford University Press, Oxford
- Reck-Peterson, S. L., Provance, D. W., Jr., Mooseker, M. S., and Mercer, J. A. (1999) *Biochim. Biophys. Acta.* **1496**, 36–51
- Cheney, R. E., and Mooseker, M. S. (1992) *Curr. Opin. Cell Biol.* **4**, 27–35
- Cheney, R. E., O'Shea, M. K., Heuser, J. E., Coelho, M. V., Wolenski, J. S., Espreafico, E. M., Forscher, P., Larson, R. E., and Mooseker, M. S. (1993) *Cell* **75**, 13–23
- Mehta, A. D., Rock, R. S., Ridf, M., Spudich, J. A., Mooseker, M. S., and Cheney, R. E. (1999) *Nature* **400**, 590–593
- Sakamoto, T., Amitani, I., Yokota, E., and Ando, T. (2000) *Biochem. Biophys. Res. Commun.* **272**, 586–590
- Walker, M. L., Burgess, S. A., Sellers, J. R., Wang, F., Hammer, J. A., III, Trinick, J., and Knight, P. J. (2000) *Nature* **405**, 804–807
- Veigel, C., Wang, F., Bartoo, M. L., Sellers, J. R., and Molloy, J. E. (2001) *Nat. Cell Biol.* **4**, 59–65
- De La Cruz, E. M., Wells, A. L., Rosenfeld, S. S., Ostap, E. M., and Sweeney, H. L. (1999) *Proc. Natl. Acad. Sci. U. S. A.* **96**, 13726–13731
- Harris, D. E., and Warshaw, D. M. (1993) *J. Biol. Chem.* **268**, 14764–14768
- Uyeda, T. Q. P., Warrick, H. M., Kron, S. J., and Spudich, J. A. (1991) *Nature* **352**, 307–311
- Wang, F., Chen, L., Arcucci, O., Harvey, E. V., Bowers, B., Xu, Y., Hammer, J. A., III, and Sellers, J. R. (2000) *J. Biol. Chem.* **275**, 4329–4335
- Spudich, J. A., and Watt, S. (1971) *J. Biol. Chem.* **246**, 4866–4871
- Veigel, C., Bartoo, M. L., White, D. C., Sparrow, J. C., and Molloy, J. E. (1998) *Biophys. J.* **75**, 1424–1438
- Homsher, E., Wang, F., and Sellers, J. R. (1992) *Am. J. Physiol. Cell Physiol.* **262**, C714–C723
- Molloy, J. E., Burns, J. E., Kendrick-Jones, J., Tregear, R. T., and White, D. C. S. (1995) *Nature* **378**, 209–212
- Uber, A., and Branton, D. (1980) *J. Ultrastruct. Res.* **71**, 95–102
- Purcell, T. J., Morris, C., Spudich, J. A., and Sweeney, H. L. (2002) *Proc. Natl. Acad. Sci. U. S. A.* **99**, 14159–14164
- Howard, J., Hudspeth, A. J., and Vale, R. D. (1989) *Nature* **342**, 154–158
- Tanaka, H., Homma, K., Iwane, A. H., Katayama, E., Ikebe, R., Saito, J., Yanagida, T., and Ikebe, M. (2002) *Nature* **415**, 192–195
- Espindola, F. S., Suter, D. M., Partata, L. B., Cao, T., Wolenski, J. S., Cheney, R. E., King, S. M., and Mooseker, M. S. (2000) *Cell Motil. Cytoskeleton* **47**, 269–281
- Warshaw, D. M., Guilford, W. H., Freyzon, Y., Kremntsova, E., Palmiter, K. A., Tyska, M. J., Baker, J. E., and Trybus, K. M. (2000) *J. Biol. Chem.* **275**, 37167–37172
- Rief, M., Rock, R. S., Mehta, A. D., Mooseker, M. S., Cheney, R. E., and Spudich, J. A. (2000) *Proc. Natl. Acad. Sci. U. S. A.* **97**, 9482–9486
- Ruff, C., Furch, M., Brenner, B., Manstein, D. J., and Meyhofer, E. (2001) *Nat. Struct. Biol.* **8**, 226–229
- Schott, D. H., Collins, R. N., and Bretscher, A. (2002) *J. Cell Biol.* **156**, 35–39
- Sata, M., Matsuura, M., and Ikebe, M. (1996) *Biochemistry* **35**, 11113–11118
- Trybus, K. M., Freyzon, Y., Faust, L. Z., and Sweeney, H. L. (1997) *Proc. Natl. Acad. Sci. U. S. A.* **94**, 48–52
- Lauzon, A. M., Fagnant, P. M., Warshaw, D. M., and Trybus, K. M. (2001) *Biophys. J.* **80**, 1900–1904
- Trybus, K. M., and Lowey, S. (1987) *J. Cell Biol.* **105**, 3007–3019
- Craig, R., and Megerman, J. (1977) *J. Cell Biol.* **75**, 990–996